Supplementary Information

Influence of Oil Composition on the Transformation, Bioaccessibility, and Intestinal Absorption of Curcumin in Nanostructured Lipid Carriers

Jin Feng,[a] Meigui Huang,[b] Zhi Chai,[c] Chunyang Li,[c] Wuyang Huang,[c] Li Cui,[c] and Ying Li[a,*]

[a] State Key Laboratory of Food Science and Technology, Jiangnan University, 1800 Lihu Road, Wuxi 214122, China

[b] Department of food science and engineering, College of light industry and food engineering, Nanjing forestry university, 159 Longpan Road, Nanjing 210037, China

[c] Institute of Agro-product Processing, Jiangsu Academy of Agricultural Sciences, 50 Zhongling Street, Nanjing 210014, China

Free fatty acids (FFAs) analyses.

One milliliter of raw digesta (for determining the released FFAs) or micelle phase (for determining the micellized FFAs), 1 mL of ethanol, 3 mL of *n*-hexane, and 0.2 mL of 2.5 M sulfuric acid (added to promote FFAs protonation) were vortexed vigorously for 10 min and sonicated in a water bath for 30 min. After that, the *n*-hexane phase was isolated by centrifugation. Two milliliters of *n*-hexane were added to the aqueous phase and the extraction was repeated as described above. The collected *n*-hexane phase was combined and an appropriate amount of powdered anhydrous Na_2SO_4 was added to remove trace water. Afterward, the organic phase was evaporated affording lipid mixture of FFAs, MAGs, TAGs, etc.

FFAs in the lipid mixture was separated on TLC plates using *n*-hexane, ethyl acetate, and acetic acid (9:1:0.1, v/v/v) as mobile phase. First, the silica gel plates were cut into 20 cm × 20 cm pieces, which were activated by incubating at 103 °C for 1 h and cooled to the room temperature in a desiccator. The lipid mixture was dissolved by a small volume of *n*-hexane and then spotted on the baseline of the plate (15 mm from the bottom) with glass capillary tubes (0.5 mm × 100 mm). C_{18}, glyceryl monostearate, glyceryl distearate, and GTS were utilized as standards to determine the position of FFAs, MAGs, di-acylglycerols (DAGs), and TAGs. The plate was allowed to develop in a TLC chamber after pre-saturated with the vapor of the mobile phase. The solvent was permitted to move up to 20 mm from the upper edge. Thereafter, the plate was air-dried at ambient temperature, and a thin slice was cut from the plate for visualization. The 2',7'-dichlorofluorescein solution (in ethanol, 2 g/L) was sprayed uniformly over

the slice with a sprayer and the slice was dried completely by a hot air gun, which was then visualized in an UV chamber at 254 nm. The bands in the slice were compared with those of the standards to identify FFAs, MAGs, DAGs, and TAGs. In general, the bands, from top to bottom, were TAGs, FFAs, DAGs, and MAGs. The silica gel corresponding to the FFAs band in the plate was carefully scrapped and collected in a round-bottom flask. The FFAs in the silica gel were extracted with 15 mL of *n*-hexane under sonication three times, and the organic phase was collected and evaporated to dryness.

FAMEs were prepared using the BF_3-MeOH method. Two milliliters of BF_3 in methanol solution (14%) was added to the aforementioned FFAs, which was allowed to react at 80 ± 1 °C for 30 min. Thereafter, 4 mL of saturated NaCl solution and 6 mL of *n*-hexane were added and mixed thoroughly. The organic phase was isolated and dried by Na_2SO_4, which was then brought to 10 mL with *n*-hexane in a volumetric flask.

GC-MS analysis was carried out using a GCMS-QP2020 instrument (Shimadzu, Japan) coupled with an Agilent HP-88 capillary column (100 m × 0.25 mm × 0.20 μm). The initial column temperature was 40 °C and held for 2 min, raised from 40 °C to 200 °C at a rate of 5 °C/min and held for 1 min, finally increased to 240 °C at a rate of 10 °C/min and kept at this temperature for 5 min. The injection temperature was set at 260 °C. Helium was used as the carrier gas with a flow rate of 1.0 mL/min. One μL of the derivatized sample was injected with a solvent delay time of 13 min and split ratio of 10 :1. The ionization was carried out in the electron impact (EI) mode at 70 eV. The

MS data were acquired in full scan mode from *m/z* 40 to 500 with an acquisition frequency of 12.8 scans per second. FAMEs were identified by comparing their retention times with those of the standards. The content of each FAME was calculated by the calibration curve of the corresponding standard.

During the simulated digestion, the residual TAGs (MCT and/or GTS) in the digesta at each time point was calculated on the basis of the amount of released FFAs and stoichiometric reaction for TAG lipolysis [1]:

$$1\ TAG + 2\ H_2O = MAG + 2\ FFA$$

Herein, the molecular weight of MCT was averagely 508.17 Da because it contained 55.50% caprylic triglyceride and 44.50% capric triglyceride.

HPLC analysis for Cur and its metabolites. An Agilent 1290 Infinity LC coupled with a diode array detector (DAD) and a Zorbax eclipse analytical XDB-C_{18} column (4.6×150 mm, 5 μm) was utilized for the quantification of Cur and its metabolisms. The injection volume was 2.0 μL and column temperature was maintained at 30 °C in an Agilent column oven. Mobile phase A was 2.00% acetic acid in water, and mobile phase B was acetonitrile. The gradients elution was as follows: 0-3 min, 30% B; 3-15 min, 30-45% B; 15-20 min, 45% B; 20-35 min, 45-70%; 35-37 min, 70% B; 37-38 min, 70-30% B. The flow rate was set at 1.0 mL/min, and the detection wavelength was 420 nm for Cur while 280 nm for HHC and OHC, respectively. Peaks were identified by comparing retention times with those of the authentic standards. Calibration curve with fine linearity was constructed by plotting the concentrations of standard solutions with their response values.

Table S1 D_Z, ζ-potential, and PDI of the NLCs.

NLCs	D_Z (nm)	ζ-potential (mV)	PDI
NLC_0	153.71 ± 4.32 a	-22.92 ± 0.29 b	0.22 ± 0.03 b
NLC_{10}	181.23 ± 4.46 b	-23.41 ± 3.43 b	0.15 ± 0.01 a
NLC_{20}	185.32 ± 3.27 b	-27.13 ± 2.98 a	0.28 ± 0.02 c
NLC_{40}	223.56 ± 10.43 c	-26.52 ± 1.11 a	0.24 ± 0.04 bc
NLC_{60}	221.23 ± 5.34 c	-26.18 ± 2 .12 a	0.17 ± 0.11 abc
NLC_{100}	189.35 ± 12.34 b	-26.15 ± 0 .53 a	0.21 ± 0.06 abc

Data are mean ± SD of three independent tests. Different lowercase letters in the same column represent significant differences ($P < 0.05$).

Table S2 Summary of the thermodynamic parameters of NLCs.

NLCs	$T_{m(\alpha)onset}$ (°C)	$T_{m(\alpha)peak}$ (°C)	$\Delta H_{m(\alpha)}$ (J/g)	$T_{m(\beta)onset}$ (°C)	$T_{m(\beta)peak}$ (°C)	$\Delta H_{m(\beta)}$ (J/g)	$T_{c\ onset}$ (°C)	$T_{c\ peak}$ (°C)	ΔH_c (J/g)
NLC_0	50.29 ± 0.12 e	56.09 ± 0.04 e	6.30 ± 0.09 e	65.57 ± 0.23 e	70.18 ± 0.15 e	0.55 ± 0.03 b	35.21 ± 0.08 c	32.33 ± 0.05 e	-8.08 ± 0.36 a
NLC_{10}	48.21 ± 1.01 d	53.23 ± 0.21 d	5.62 ± 0.16 d	64.32 ± 0.15 d	68.43 ± 0.34 d	1.10 ± 0.07 d	32.34 ± 1.11 b	28.12 ± 1.12 d	-7.61 ± 0.42 b
NLC_{20}	44.56 ± 0.33 c	48.98 ± 0.32 c	3.63 ± 0.78 c	63.45 ± 0.57 c	67.43 ± 0.54 c	1.82 ± 0.55 e	31.33 ± 0.87 b	26.08 ± 0.43 c	-5.96 ± 0.23 c
NLC_{40}	41.23 ± 0.79 b	46.56 ± 0.15 b	0.95 ± 0.02 b	62.76 ± 0.35 b	65.10 ± 0.03 b	0.43 ± 0.02 a	27.52 ± 1.04 a	23.76 ± 0.11 b	-2.29 ± 0.03 d
NLC_{60}	39.32 ± 0.03 a	43.45 ± 0.09 a	0.16 ± 0.01 a	61.34 ± 0.14 a	64.12 ± 0.12 a	0.78 ± 0.09 c	26.43 ± 0.13 a	22.12 ± 0.08 a	-1.16 ± 0.06 e
NLC_{100}	n.d.	n.d.	n.d.	n.d.	n.d.	n.d.	n.d.	n.d.	n.d.

[a]All measurements were performed within 1 h after preparation.

N.d. = not detected: NLC_{100} did not crystallize during the heating–cooling process.

Data are mean ± SD of three independent tests. Different lowercase letters in the same column represent significant differences ($P < 0.05$).

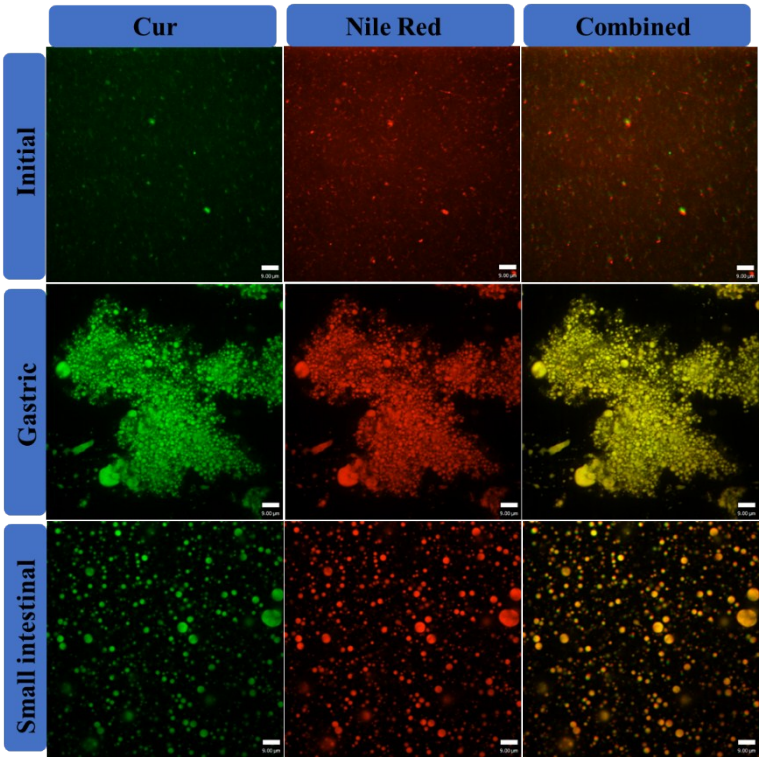

Fig. S1. CLSM images of NLC_0 at various stages of the simulated digestion. Bar: 9 μm.

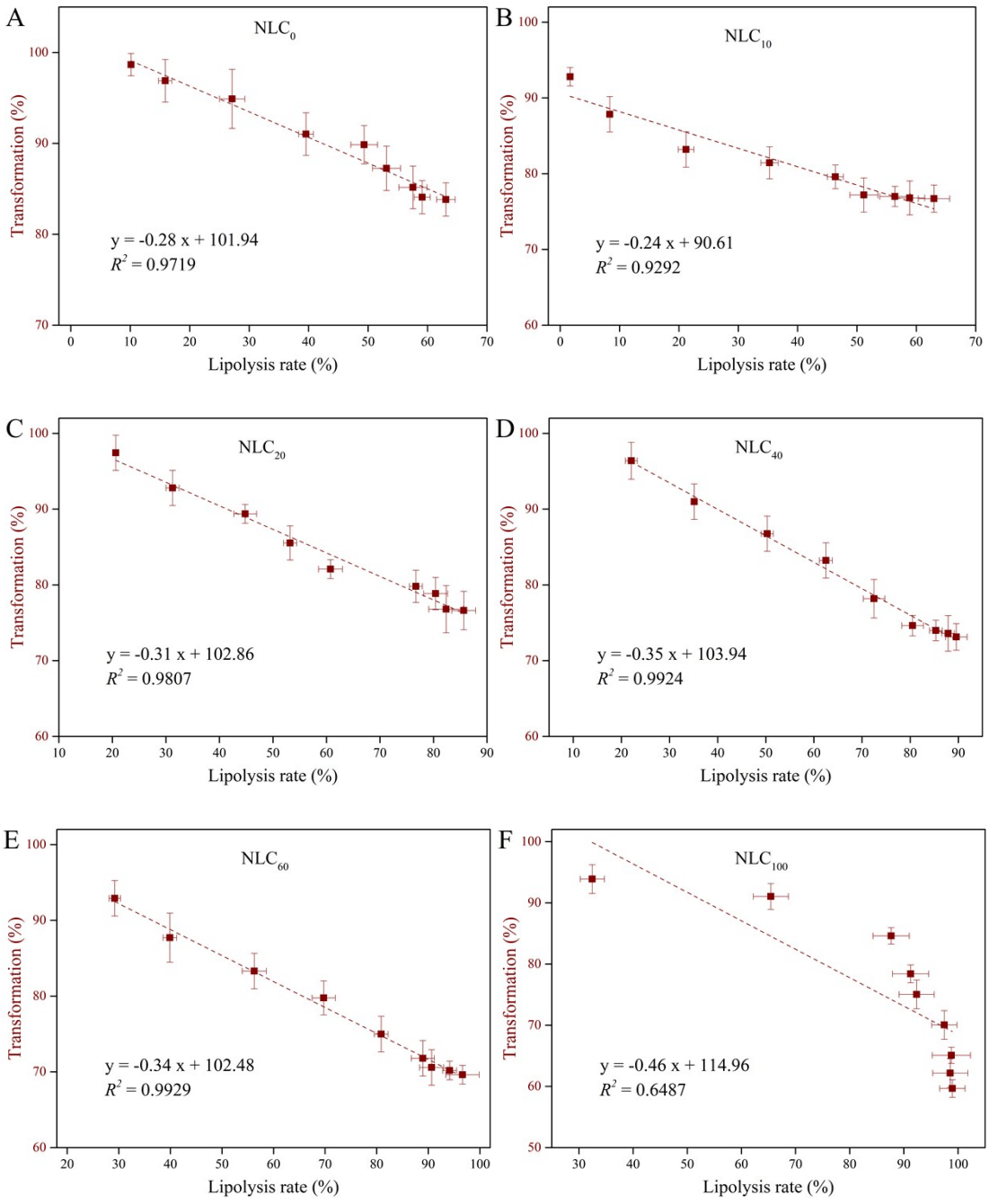

Fig. S2. Relationship between Cur transformation and lipolysis rates of NLCs during the small intestinal digestion. The dash lines were drawn using linear regression.

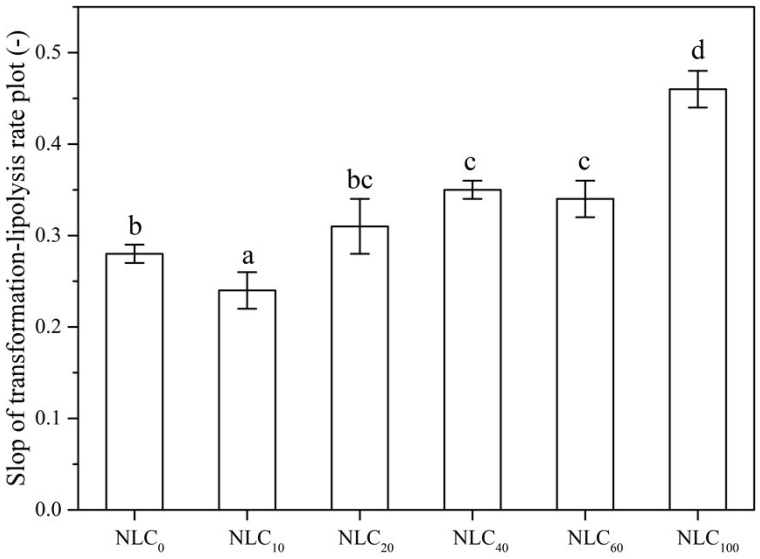

Fig. S3. Slops of the transformation-lipolysis rate plot. Different lowercase letters represent significant differences ($P < 0.05$).

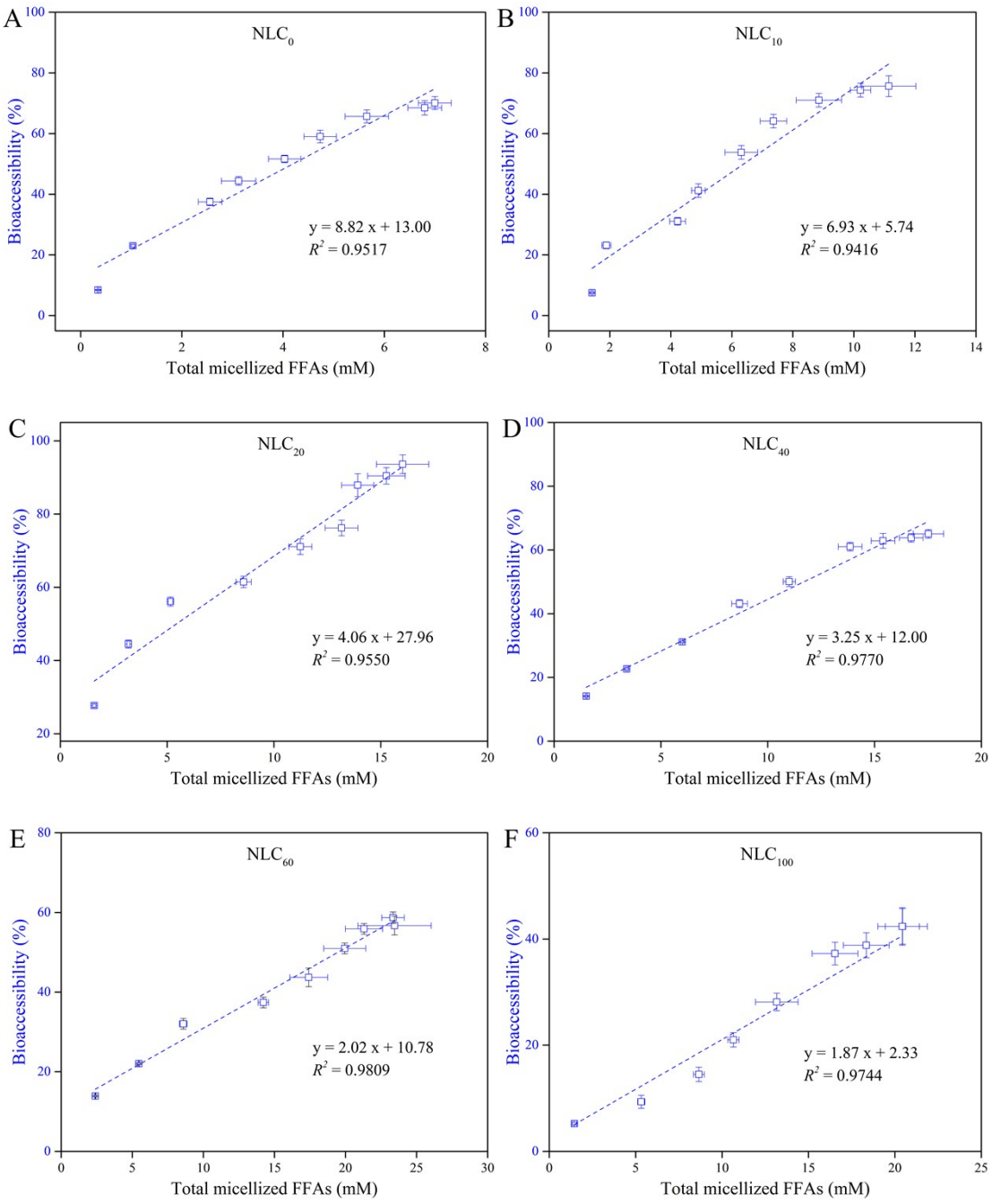

Fig. S4. Relationship between Cur bioaccessibility and total micellized FFAs during the small intestinal digestion. The dash lines were drawn using linear regression.

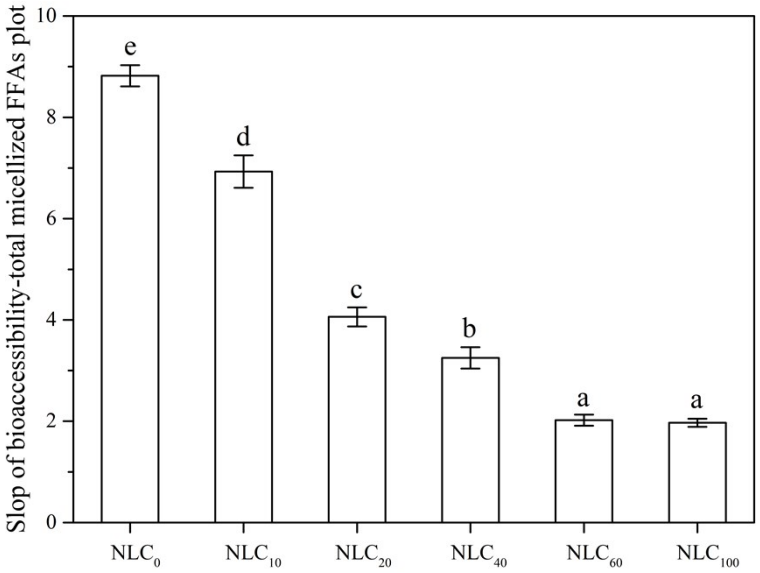

Fig. S5. Slops of the bioaccessibility-total micellized FFAs plot. Different lowercase letters represent significant differences ($P < 0.05$).

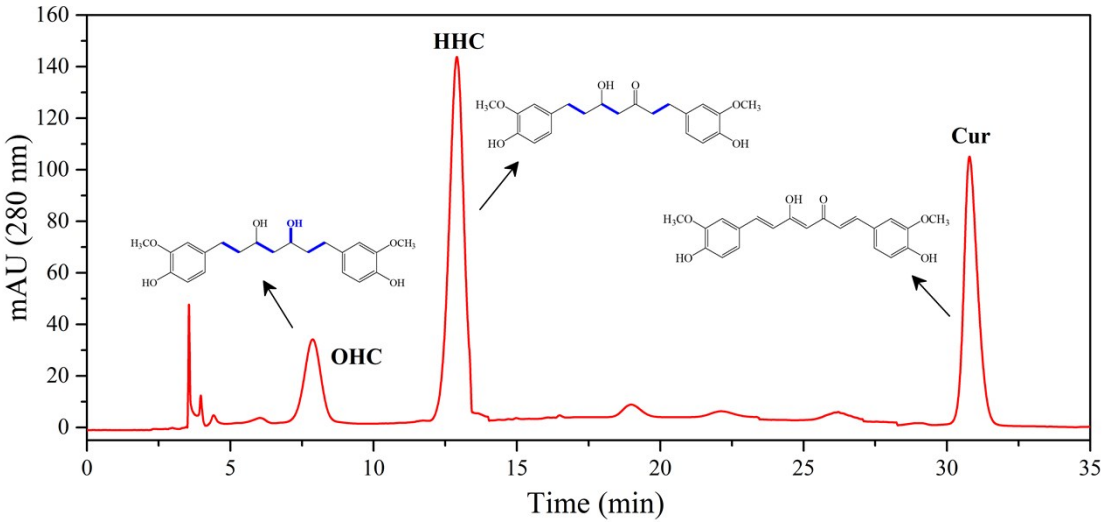

Fig. S6. Typical HPLC profiles of Cur and its reductive metabolites (HHC and OHC) extracted from the BP medium of the Caco-2 monolayer models after conjugate hydrolysis with β-glucuronidase and sulfatase.

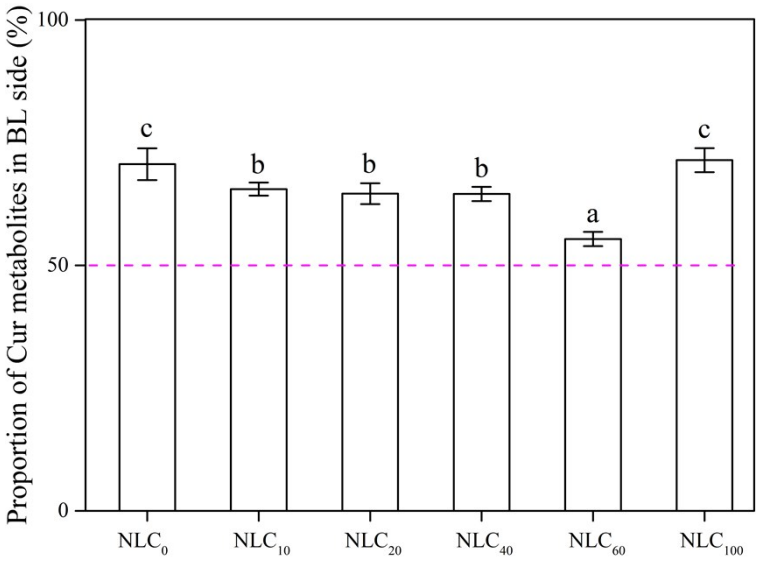

Fig. S7. Proportion of Cur metabolites in relation to the total compounds in the BL side of Caco-2 monolayers after 4 h incubation with micellar Cur isolated from the digesta of different NLCs. Different lowercase letters represent significant differences ($P < 0.05$).

1. Y. Liand D. J. McClements, New mathematical model for interpreting ph-stat digestion profiles: Impact of lipid droplet characteristics on in vitro digestibility, *J. Agric. Food Chem.*, 2010, **58**, 8085-8092.